INDIAN INSTITUTE OF TECHNOLOGY BOMBAY

AERODYNAMICS OF COMPRESSORS AND TURBINES

AE 651

Design of Transonic Axial Fan

Report By:
Panshikar Anay Rajan - 18D180020
Avinash Arun - 180010016

Under the guidance of Prof. A. M. Pradeep

December 9, 2020

Contents

1 Introduction

1.1 Axial Flow Compressors

Axial Flow Compressors are characterized by flow majorly parallel to the axis of rotation. Axial compressors can consist of many stages. One stage of an axial compressor consist of a rotating component called the **Rotor** and a stationary component **Stator**. The compression occurs both in the rotor as well as the stator. The axial compressor compresses the working fluid by first accelerating the air and then diffusing it to obtain a static pressure increase. The air is accelerated in the rotor and then diffused in the stator. Per stage pressure ratio is limited because a compressor operates in an adverse pressure gradient environment. The rotor blade motion gives rise to 2 distinct velocity components- absolute and relative. In the rotor, the relative velocity decreases and hence there is diffusion w.r.t. the relative velocity. Flow analysis is carried out using velocity triangles as shown in *Figure 1*[1]. The fan in turbofan engines is also an axial compression

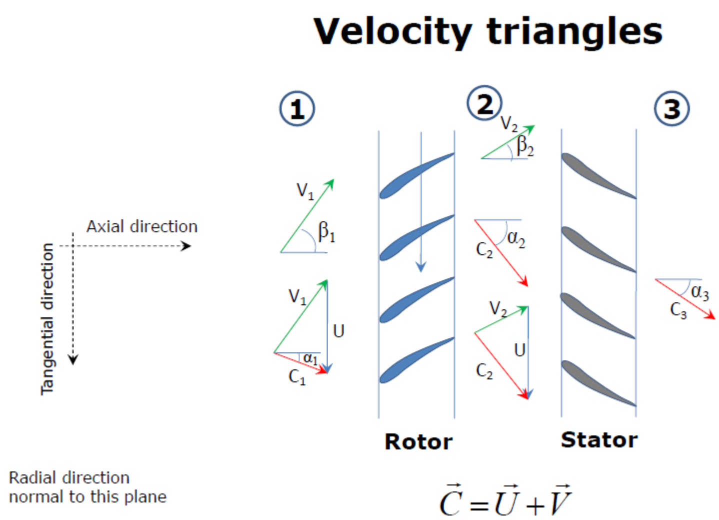

Figure 1: Velocity triangles for axial compressor

module which is treated as an axial compressor having a fewer number of blades of **very large height, wide chord, and large twist**. Based on flow regime in the compressor, it may be classified as a subsonic, transonic and supersonic compressor.

1.2 Transonic Axial Compressors

A **Transonic Axial Compressor** is characterized by subsonic mach number near the hub, sonic mach at the mean radius and supersonic mach at the tip. Transonic axial flow compressors are fundamental components in aircraft engines as they make it possible to maximize pressure ratios per stage unit. Performance of transonic compressors has today reached a high level but engine manufacturers are oriented towards increasing it further. A small increment in efficiency, for instance, can result in huge savings in fuel costs and determine a key factor for product success.
The flow field that develops inside a transonic compressor rotor is extremely complex and presents many challenges to compressor designers, who have to deal with several and concurring flow features such as **shock waves, shock/boundary layer interaction, intense secondary flows**, etc., inducing energy losses and efficiency reduction[2].

[1]Class lecture slides, "Aerodynamics of Compressors and Turbines"
[2]"Recent advances in transonic axial compressor aerodynamics", Roberto Biollo, Ernesto Benini

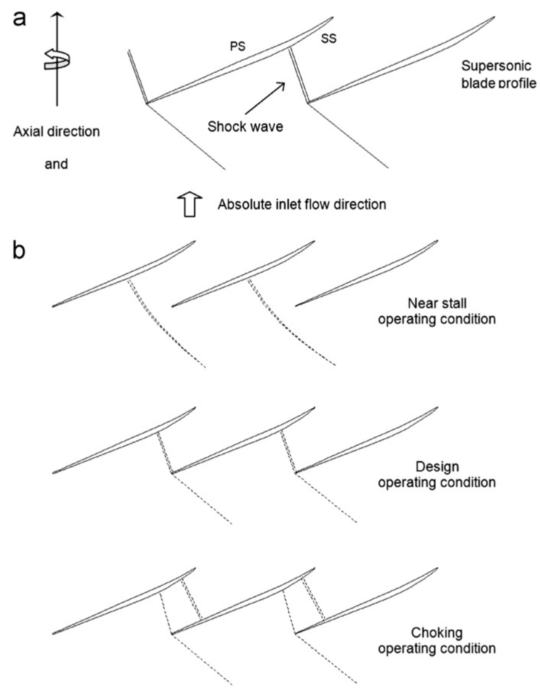

Figure 2: Shock wave configuration inside transonic compressor

2 Design of Single Stage Transonic Axial Fan

2.1 Problem Statement

Design a single-stage transonic axial fan for the given specifications-

Pressure Ratio, π_c	1.6
Outer Diameter (m)	0.8
Hub to tip ratio	0.4
Rotor speed, N (rpm)	9500
Massflow Rate, $\dot{m}$ (kg/s)	24

2.2 Design Criteria

The transonic fan stage needs to satisfy some parametric criteria for its efficient functioning. They are stated as follows-

- ΔT_0 **= 45-55K**
  The total temperature rise of the transonic stage is to be kept within this limit as per literature. If the rise is being either far beyond this range or much lower than this range, then the stage is more likely to become a supersonic or subsonic stage respectively.

- $((M_1)_{rel})_{tip}$ **= 1.1-1.7**
  The tip relative Mach number is to be kept within the above range. An increase above the upper threshold leads to unnecessary shock effects, leading to drastic efficiency drop.

- **Hub to tip ratio $\leq$ 0.4**
  Since fans tend to handle larger mass flowrates, the hub to tip ratio is usually kept low and it is seen that the given specification itself is meeting this criteria by default.

- M_a **Axial Mach Number = 0.4-0.7**
  The axial Mach number is to be kept in the above range. Alleviation from this design limit might lead to incidence losses.

2.3 Design Procedure

We will use the open-source, CFD based Turbomachinery software **Multall** for the design of the fan. The input to this are our given parameters and some assumed ones to initiate the process after satisfying the design criteria. First we will run the **meangen** script to obtain the velocity triangles at one radial location and verify the obtained values by cross-checking with the values obtained via an **Excel** spreadsheet. Then we can move forward to generate the blade shapes to obtain the complete stage via the **stagen** script. Then we will use the **multall-open** script to run the simulation until the inflow and outflow mass rates converge. Lastly, we will use a CAD software to develop the 2D and 3D blade profiles.

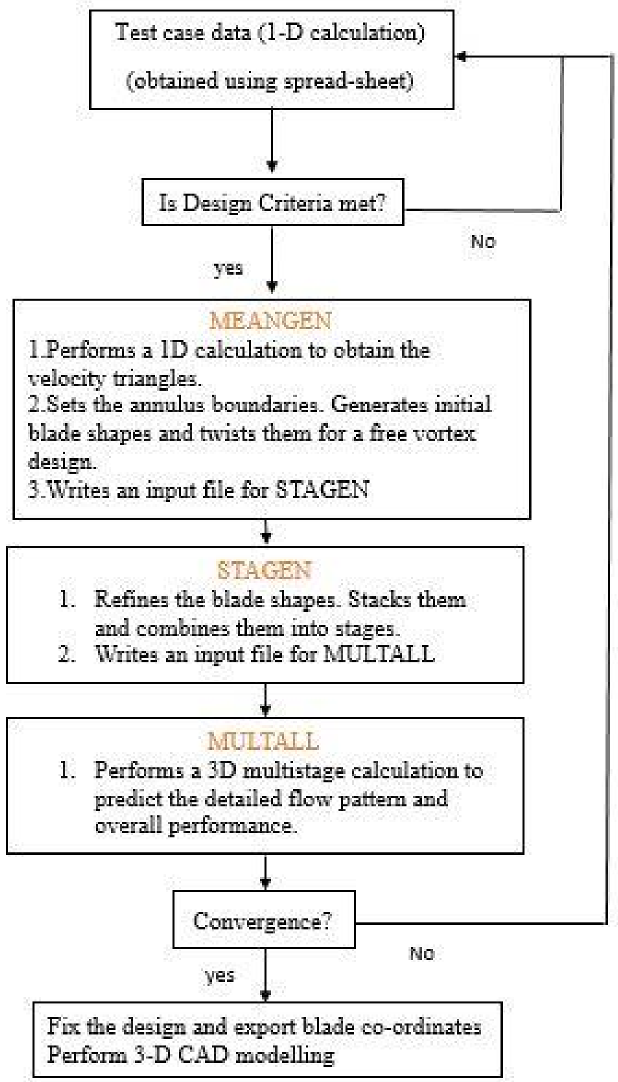

Figure 3: Design Process

3 Meanline Design

3.1 Given parameters

Pressure Ratio, π_c	1.6
Outer Diameter (m)	0.8
Hub to tip ratio	0.4
Rotor speed, N (rpm)	9500
Massflow Rate, $\dot{m}$ (kg/s)	24

3.2 Assumed parameters

Based on the design criteria, we assume some more initial parameters to begin the process.

Inlet Static Temperature, T_1 (K)	300
Inlet Mach Number, M_1	0.5
Isentropic Efficiency, η_{is}	0.9
No IGV, α_1	0°

3.3 Estimation of remaining parameters

Using the above specified parameters, we will calculate the other required design parameters at the mean radius.

- Inlet density, ρ_1:

$$\rho_1 = \frac{\dot{m}}{A_1 C_a}$$

- Inlet Area, A_1:

$$A_1 = \frac{\pi(d_t^2 - d_h^2)}{4}$$

- Inlet axial absolute velocity, $C_1 = C_a$:

$$C_1 = C_a = M_1\sqrt{\gamma R T_1}$$

- Inlet Pressure, P_1:

$$P_1 = \rho_1 R T_1$$

- Blade speed at mean diameter, U_m:

$$U_m = \frac{\pi N d_m}{60}$$

- Inlet blade angle, β_1:

$$\beta_1 = tan^{-1}(\frac{U_m}{C_a})$$

- Enthalpy change across the stage, Δh_0:

$$\Delta h_0 = \frac{C_p T_{01}}{\eta_{is}}(\pi_c^{\frac{\gamma-1}{\gamma}} - 1)$$

- Exit absolute velocity angle can be found by equating Aerodynamic work to change in enthalpy (assuming axial velocity constant):

$$\alpha_2 = tan^{-1}(\frac{\Delta h_0}{U_m C_a} + tan(\alpha_1))$$

- Exit blade angle, β_2:

$$\beta_2 = tan^{-1}(\frac{U_m}{C_a} - tan(\alpha_2))$$

- Flow coefficient, ϕ:

$$\phi = \frac{C_a}{U_m}$$

- Stage Loading Coefficient, Ψ:

$$\Psi = \frac{\Delta h_0}{U_m^2}$$

- Degree of Reaction, R_x:

$$R_x = \frac{C_a}{2U_m}(tan(\beta_1) + tan(\beta_2))$$

- Diffusion factor for Rotor and Stator:

$$D^*_{Rotor} = 1 - \frac{V_2}{V_1} + \frac{|V_{w1} - V_{w2}|}{2(\frac{C}{S})V_1}$$

$$D^*_{Stator} = 1 - \frac{C_2}{C_1} + \frac{|C_{w1} - C_{w2}|}{2(\frac{C}{S})C_1}$$

The design calculations are done using the **meangen** script of Multall by first estimating the above mentioned parameters and then verifying the same by the formulae. We proceed when there is a match between the meangen and the calculated values. The final parameter values at mean radius are shown below. (Meangen output is provided in the Appendix)

- Inlet density, $\rho_1 = 0.327 kg/m^3$
- Inlet Area, $A_1 = 0.422 m^2$
- Inlet axial absolute velocity, $C_1 = C_a = 173.639 m/s$
- Inlet Absolute Mach Number, $M_1 = 0.5$
- Inlet Pressure, $P_1 = 28199.61$ Pa
- Blade speed at mean diameter, $U_m = 278.555 m/s$
- Inlet blade angle, $\beta_1 = 58.0622°$
- Enthalpy change across the stage, $\Delta h_0 = 50555.026 J/kg$
- Total temperature difference across stage, $\Delta T_0 = 50.3023$ K
- Exit absolute velocity angle, $\alpha_2 = 46.266°$
- Exit blade angle, $\beta_2 = 29.205°$
- Flow coefficient, $\phi = 0.623$
- Stage Loading Coefficient, $\Psi = 0.652$
- Degree of Reaction, $R_x = 0.674$
- Diffusion factor for Rotor and Stator:

$$D^*_{Rotor} = 0.532$$

$$D^*_{Stator} = 0.534$$

4 Design using Free Vortex Law

We will use the free vortex law for obtaining the value of the parameters at the other radial locations. We know that by Free Vortex Law,

$$C_w.r = constant$$

i.e. the whirl velocity component varies inversely with the radius. C_a and Δh_0 don't change along the radial direction. Using-

$$tan((\alpha_1)_r) + tan((\beta_1)_r) = \frac{U_r}{(C_a)_r}$$

we will estimate the values of α_1, β_1 and other design parameters at various radial locations using **Excel**. Simultaneously, we will also use the **stagen** script of Multall to calculate the variations along radius and compare the results. The following is the tabulation of the same-

Parameters	Sectional Radius												
	Hub						Mean						Tip
r(m)	0.16	0.18	0.2	0.22	0.24	0.26	0.28	0.3	0.32	0.34	0.36	0.38	0.4
Cw1(m/s)	0	0	0	0	0	0	0	0	0	0	0	0	0
Cw2(m/s)	317.6085	282.3187	254.0868	230.988	211.739	195.4514	181.4906	169.3912	158.8043	149.4628	141.1593	133.7299	127.0434
R(r/rm)	0.571429	0.642857	0.714286	0.785714	0.857143	0.928571	1	1.071429	1.142857	1.214286	1.285714	1.357143	1.428571
U1(m/s)	159.174	179.0708	198.9675	218.8643	238.761	258.6578	278.5545	298.4513	318.3481	338.2448	358.1416	378.0383	397.9351
U2(m/s)	159.174	179.0708	198.9675	218.8643	238.761	258.6578	278.5545	298.4513	318.3481	338.2448	358.1416	378.0383	397.9351
Rx	0.002323	0.211712	0.361487	0.472303	0.556588	0.622182	0.674228	0.716216	0.750581	0.779061	0.802928	0.823127	0.840372
Ca1(m/s)	173.6397	173.6397	173.6397	173.6397	173.6397	173.6397	173.6397	173.6397	173.6397	173.6397	173.6397	173.6397	173.6397
Ca2(m/s)	173.6397	173.6397	173.6397	173.6397	173.6397	173.6397	173.6397	173.6397	173.6397	173.6397	173.6397	173.6397	173.6397
delT0(K)	50.30226	50.30226	50.30226	50.30226	50.30226	50.30226	50.30226	50.30226	50.30226	50.30226	50.30226	50.30226	50.30226
UdelCw(J/kg)	50555.03	50555.03	50555.03	50555.03	50555.03	50555.03	50555.03	50555.03	50555.03	50555.03	50555.03	50555.03	50555.03
alpha1	0	0	0	0	0	0	0	0	0	0	0	0	0
alpha2	61.33414	58.40646	55.65179	53.06686	50.64603	48.382	46.26643	44.29042	42.44485	40.72069	39.10917	37.60193	36.19105
beta1	42.51122	45.88218	48.88867	51.57267	53.97336	56.12612	58.06224	59.80905	61.39019	62.82607	64.13425	65.32984	66.42586
beta2	-42.3783	-30.7361	-17.6112	-3.99397	8.845491	20.00196	29.20503	36.62208	42.57745	47.39247	51.33151	54.59708	57.3404
beta1-beta2	84.88955	76.61831	66.49992	55.56665	45.12787	36.12416	28.85721	23.18697	18.81274	15.4336	12.80274	10.73276	9.085455
V1(m/s)	235.557	249.4335	264.0811	279.3785	295.2246	311.5359	328.2429	345.2882	362.6241	380.2109	398.0152	416.0093	434.1694
V2(m/s)	235.0579	202.017	182.1782	174.0624	175.7297	184.7858	198.9275	216.3499	235.8071	256.4944	277.9065	299.7288	321.7655
Vw1(m/s)	159.174	179.0708	198.9675	218.8643	238.761	258.6578	278.5545	298.4513	318.3481	338.2448	358.1416	378.0383	397.9351
Vw2(m/s)	-158.434	-103.248	-55.1193	-12.1237	27.02203	63.2064	97.06397	129.0601	159.5438	188.782	216.9822	244.3084	270.8917
C2(m/s)	361.975	331.4432	307.7513	288.9744	273.8324	261.4421	251.1764	242.5781	235.3073	229.1067	223.7783	219.1676	215.1529
flowcoeff	1.09088	0.969671	0.872704	0.793367	0.727253	0.671311	0.62336	0.581802	0.54544	0.513355	0.484835	0.459318	0.436352
stageloading	1.995354	1.576576	1.277026	1.055394	0.886824	0.755637	0.651544	0.567567	0.498838	0.441878	0.394144	0.353747	0.319257
Mrel1	0.678293	0.71825	0.760428	0.804477	0.850107	0.897076	0.945184	0.994266	1.044185	1.094827	1.146095	1.197909	1.250202

Assumed quantities
Hub
Mean
Tip

Figure 4: Design using Free Vortex Law

4.1 Variation of Flow Angles

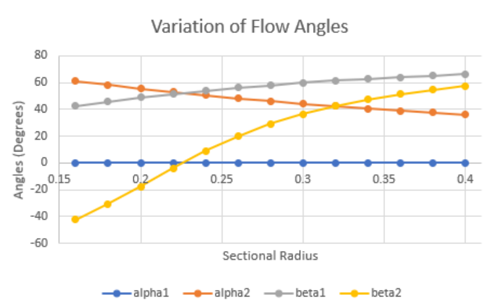

Figure 5: Flow Angles radial variation

We observe that the blade angles increase towards the tip. The flow turning $(\beta_2 - \beta_1)$ is large at the hub section. The absolute velocity angle downstream decreases.

4.2 Degree of Reaction

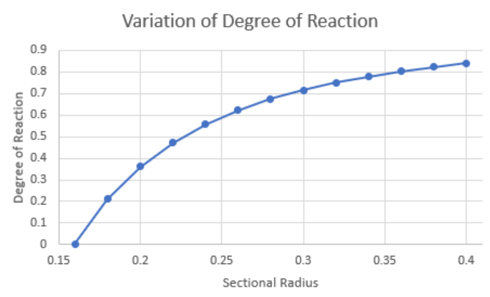

Figure 6: Degree of Reaction radial variation

The degree of Reaction will increase from hub to tip as per Free Vortex Law.

4.3 Flow Coefficient

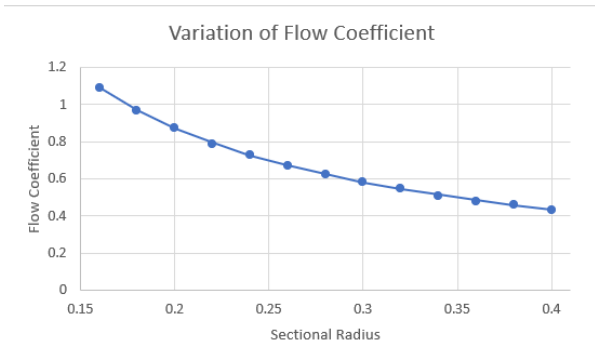

Figure 7: Flow Coefficient radial variation

The Flow coefficient will reduce from hub to tip as the axial velocity remains constant from Free Vortex Law and blade speed increases.

4.4 Stage Loading

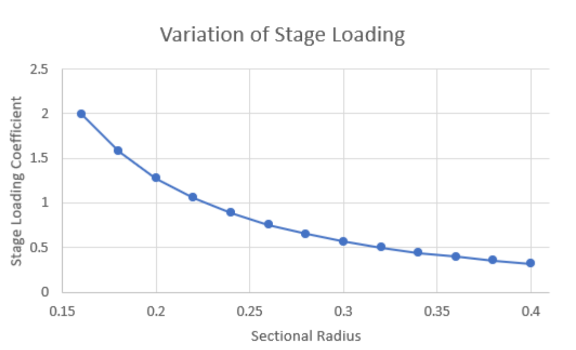

Figure 8: Stage Loading radial variation

The stage loading will also reduce towards the tip as the enthalpy change is constant by Free Vortex Law but the blade speed will increase.

4.5 Inlet Relative Mach Number

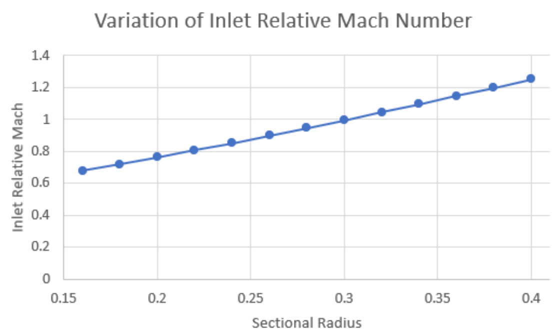

Figure 9: Inlet Relative Mach radial variation

The inlet relative mach number increases towards the tip. As per our design criteria, we observe that flow is subsonic at the hub, transonic at the mean radius and supersonic at the tip region. Also the value at the tip is within the desired limits (1.1 - 1.7).

5 Blade Geometry

The blade sections are generated using Multall. The **multall-open** script runs the simulation based on the input data until the mass inflow and outflow rates converge. Then it stores a series of y_{up} and y_{low} values for a range of x values in an output file which determines the shape of the airfoil at one radial location. Any CAD software can be used for interpreting this data and generating the 2D airfoil shape from the obtained data and subsequent 3D visualization.

5.1 Blade Design

The stored plotting data represents 6 airfoils shapes for rotor and stator hub, mean and tip respectively. We used the software **AUTODESK FUSION 360™** for visualizing the 2D blade sections and the 3D blade shapes.

5.2 Rotor

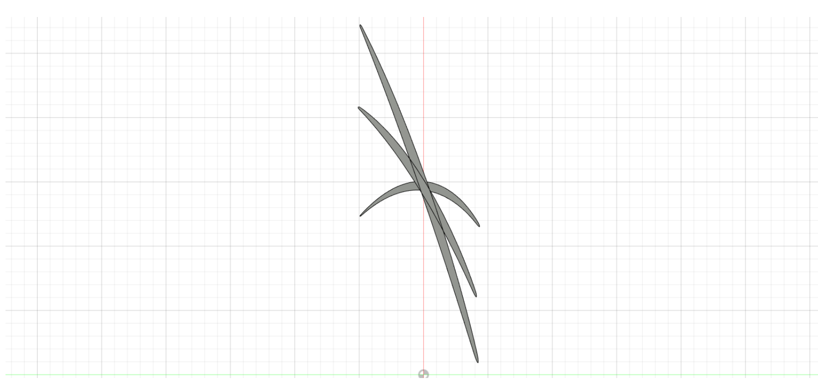

Figure 10: 2D visualizations of airfoils at hub, mean and tip

The airfoils are thin and have very high twist which will cause high flow turning.
Next the complete rotor blade was generated using these 3 airfoils shapes using the blade height and the *loft* function of Fusion 360. The rotor blade viewed from various directions is shown below.

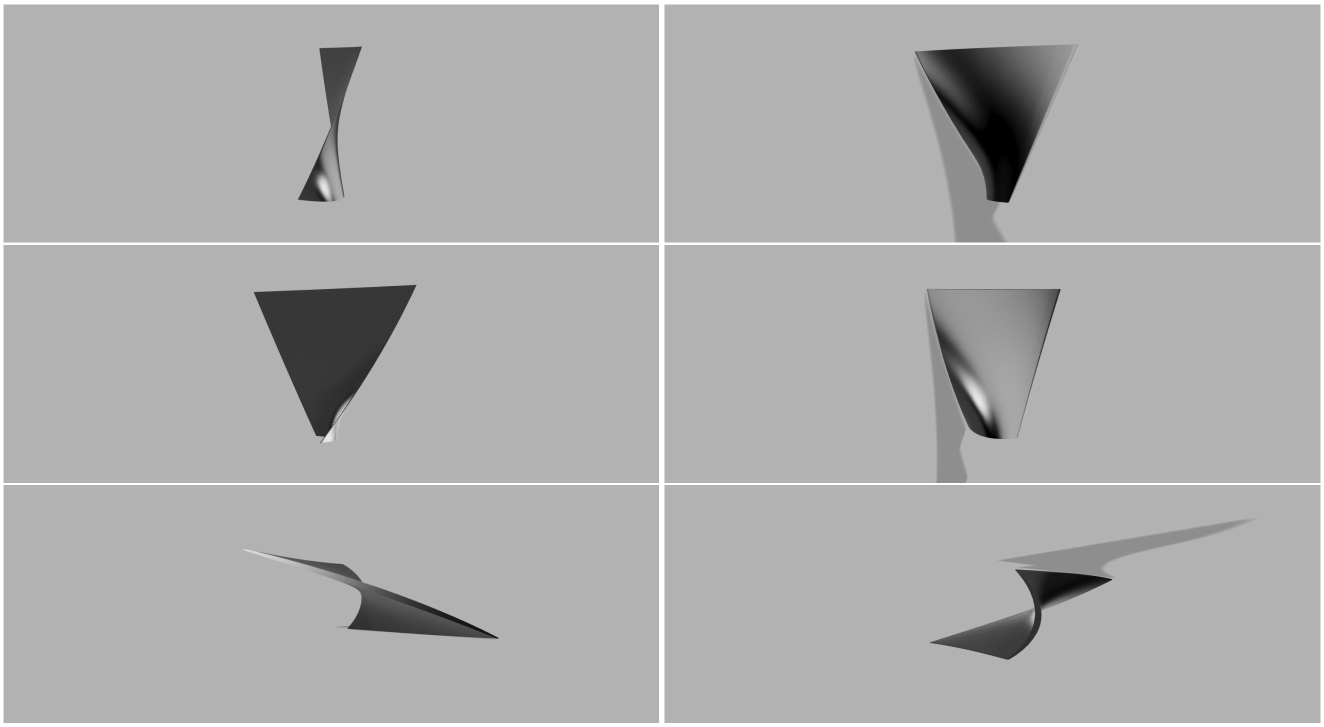

Figure 11: 3D visualization of Rotor Blade

5.3 Stator

Figure 12: 2D visualizations of airfoils at hub, mean and tip

Unlike the rotor, there is significant less twist observed for the stator. Also, the stator blades are more thicker as compared to the rotor blades.
Similar to the rotor, the stator blade was designed using the blade height and function *loft*. Its visualizations are shown below.

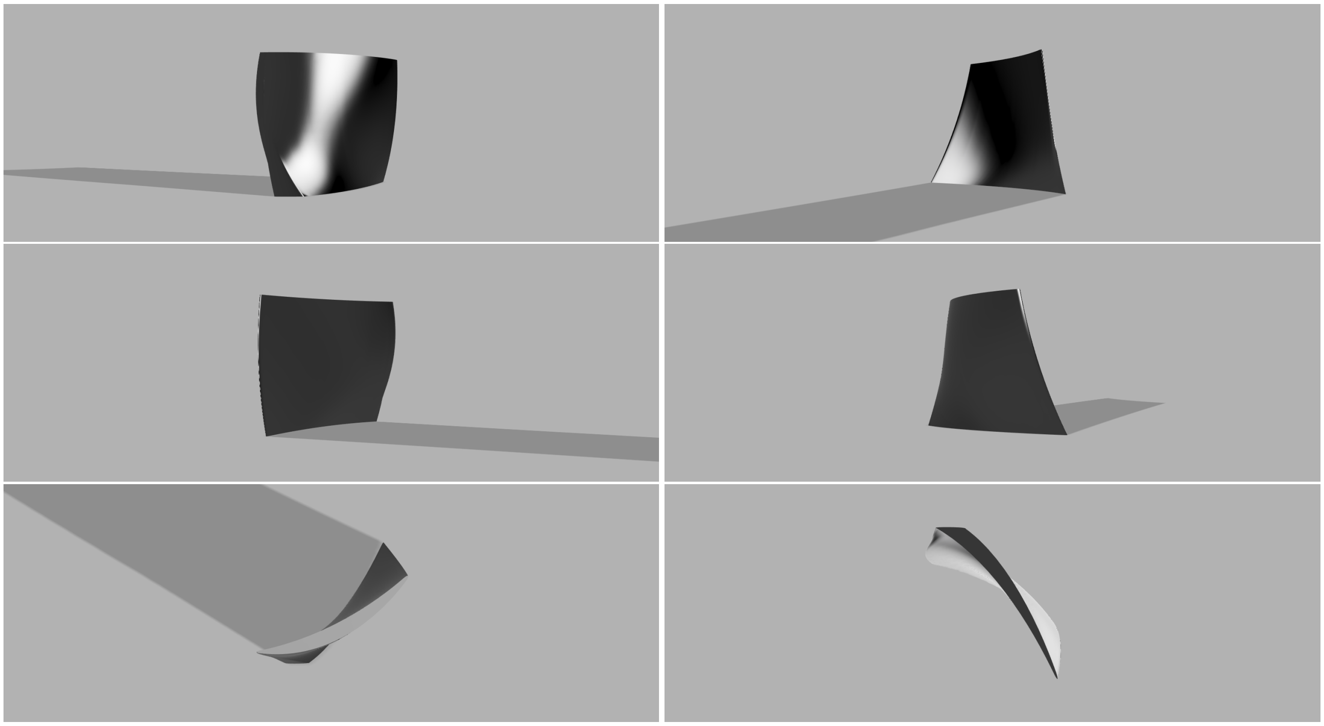

Figure 13: 3D visualization of Stator Blade

5.4 3D Fan

The complete 3D Transonic Fan was created using the rotor and stator blades designed. 50 rotor and 50 stator blades were used. (This is done just for visualization, actual blades for rotor and stator may vary depending upon blockage factor to meet the mass flow rate requirement)

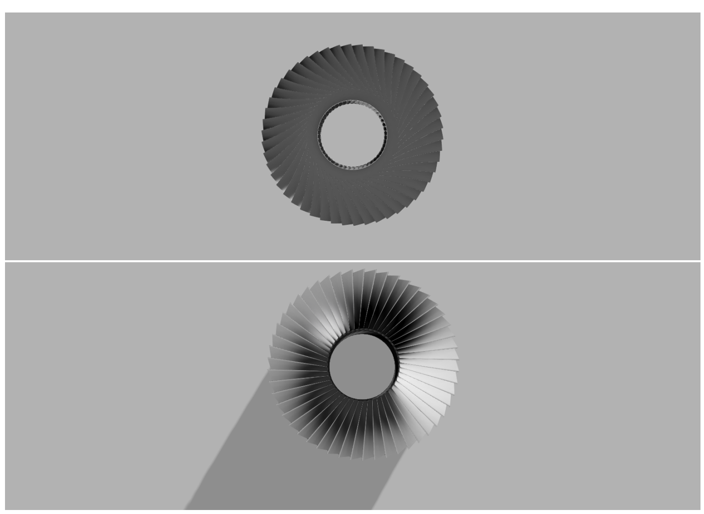

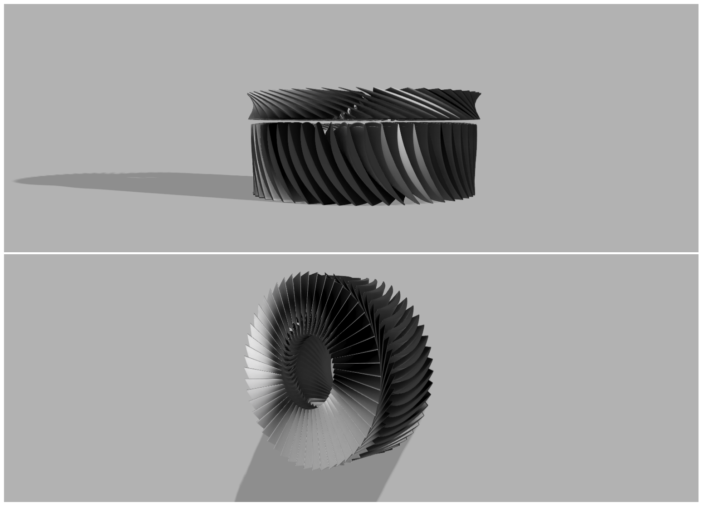

Figure 14: 3D visualization of complete Fan

An animation of the Rotor motion was also created using the CAD software. (Drive link provided in the Appendix)

6 Conclusions

- Manual calculations along with appropriate assumptions carried out for the inlet parameters to design the single-stage axial transonic fan for given specifications.
- Manual calculations done for estimating 1D flow velocity triangles and compared the results with the computations done using **meangen**.
- Computational calculations done using **stagen** to obtain the design parameters along the radius and compared the results with the manual calculations performed using **Free Vortex Law**.
- Output from the stagen given to **Multall** to perform the simulation for the stage until convergence is obtained for inflow and outflow mass rates.
- The blade profiles obtained are visualized in 2D and 3D using CAD Software **AUTODESK FUSION 360™**.
- All the design criteria for the optimum fan performance are met.
- Blade shapes obtained confirm the high chord, high twist nature of the fan blades.

7 References

- "Recent advances in transonic axial compressor aerodynamics", Roberto Biollo, Ernesto Benini, University of Padova, Dept.of Mechanical Engineering, Via Venezia 1, Padova 35131, Italy
- NPTEL, "Turbomachinery Aerodynamics", by Prof. A. M. Pradeep and Prof. Baskar Roy.
- Class lecture slides, "Aerodynamics of Compressors and Turbines", by Prof. A. M. Pradeep.
- Ahmed F. El-Sayed, Fundamentals of Aircraft and Rocket Propulsion, Springer Edition.

8 Appendix

- Output of Meangen

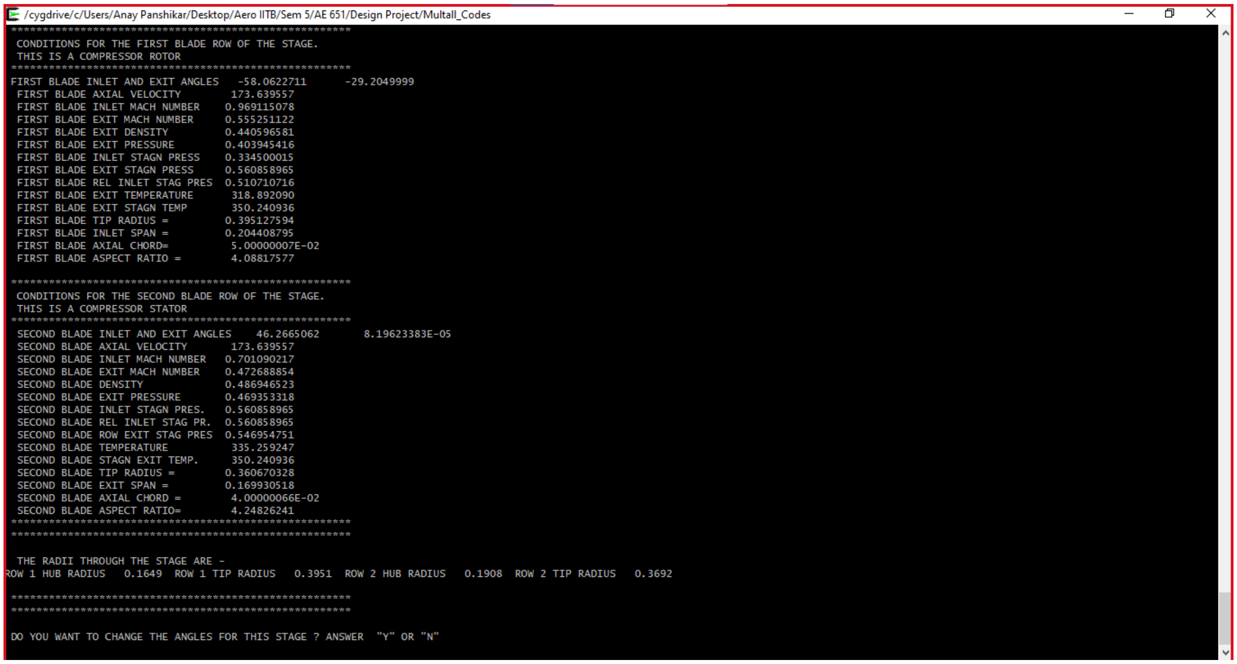

Figure 15: Meangen

- Blade geometry coordinates extracted from Multall (drive links)-

  Rotor
  Stator

- Animation of Rotor motion (drive link)-
  Rotor motion